

## Carbo-Cages: A Computational Study

Jon M. Azpiroz,<sup>†,‡</sup> Rafael Islas,<sup>‡</sup> Diego Moreno,<sup>‡</sup> María A. Fernández-Herrera,<sup>§</sup> Sudip Pan,<sup>||</sup> Pratim K. Chattaraj,<sup>||</sup> Gerardo Martínez-Guajardo,<sup>‡,⊥</sup> Jesus M. Ugalde,<sup>\*,†</sup> and Gabriel Merino<sup>\*,‡</sup>

<sup>†</sup>Kimika Fakultatea, Euskal Herriko Unibertsitatea (UPV/EHU), and Donostia International Physics Center (DIPC), P. K. 1072, 20080 Donostia, Euskadi, Spain

<sup>‡</sup>Departamento de Física Aplicada, Centro de Investigación y de Estudios Avanzados, Unidad Mérida, Km 6 Antigua Carretera a Progreso. Apdo. Postal 73, Cordemex, 97310, Mérida, Yuc., México

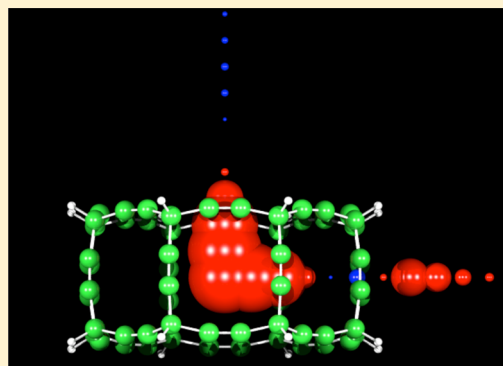
<sup>§</sup>Facultad de Ciencias Químicas, Benemérita Universidad Autónoma de Puebla, Ciudad Universitaria, 72570, Puebla, Pue., México

<sup>||</sup>Department of Chemistry and Centre for Theoretical Studies, Indian Institute of Technology, Kharagpur, 721302, India

<sup>⊥</sup>Unidad Académica de Ciencias Químicas, Área de Ciencias de la Salud, Universidad Autónoma de Zacatecas, Km. 6 carretera Zacatecas-Guadalajara s/n, Ejido La Escondida C. P. 98160, Zacatecas, Zac., Mexico

### S Supporting Information

**ABSTRACT:** Inspired by their geometrical perfection, intrinsic beauty, and particular properties of polyhedranes, a series of carbo-cages is proposed in silico via density functional theory computations. The insertion of alkynyl units into the C–C bonds of polyhedranes results in a drastic lowering of the structural strain. The induced magnetic field shows a significant delocalization around the three-membered rings. For larger rings, the response is paratropic or close to zero, suggesting a nonaromatic behavior. In the carbo-counterparts, the values of the magnetic response are shifted with respect to their parent compounds, but the aromatic/nonaromatic character remains unaltered. Finally, Born–Oppenheimer molecular dynamics simulations at 900 K do not show any drastic structural changes up to 10 ps. In the particular case of a carbo-prismane, no structural change is perceived until 2400 K. Therefore, although carbo-cages have enthalpies of formation 1 order of magnitude higher than those of their parent compounds, their future preparation and isolation should not be discarded, because the systems are kinetically stable, explaining why the similar systems like carbo-cubane have already been synthesized.



## INTRODUCTION

Polyhedranes have awoken interest in the chemical community due to their aesthetically pleasant molecular structures, challenging synthesis, sophisticated structure–energy correlation, and singular physicochemical properties. Particularly, cage-like polyhedral hydrocarbons,  $(CH)_n$ , are attractive due to their nonclassical carbon bonding,<sup>1</sup> unusual ring strain,<sup>1–9</sup>  $\sigma$ -aromaticity/antiaromaticity,<sup>3,5,10–12</sup> and their ability to participate in isomerization reactions.<sup>13,14</sup>

Illustrative examples of polyhedral hydrocarbons include prismanes and platonic hydrocarbons. The first ones, so-called  $[m,n]$ -prismanes, are built of  $m$  identical  $n$ -membered rings, held together by  $n$  single C–C bonds in a regular prism with a  $D_{nh}$  symmetry. The presence of semiplanar carbon centers and their high strain suggests that they could be used as high energy density materials and energy storage systems.<sup>1</sup> As far as we know, only triprismane,<sup>15</sup> cubane,<sup>16,17</sup> and pentaprismane<sup>18,19</sup> have been obtained experimentally. On the other hand, platonic hydrocarbons are molecular representations of the platonic solids. Tetrahedrane, cubane, and dodecahedrane are archetypal examples of such systems.

Thirty years ago, Scott et al. synthesized an interesting group of molecules called carbomers.<sup>20</sup> Carbomers result from the insertion of one or more  $-C\equiv C-$  units into the bonds of a parent compound. The simplest example of a carbomer is acetylene. The linearity of the  $-C\equiv C-$  fragments facilitates the formation of rigid structures. Furthermore, the characteristics of  $\pi$ -bonds provide interesting properties. For instance, it is shown that the incorporation of alkynyl groups enhances the optoelectronic properties of the parent molecules.<sup>21</sup> It is also predicted that the carbo analogues of the two most common carbon allotropes (graphite and diamond) exhibit promising properties. The alkynyl-expanded graphdiyne displays in silico third-order nonlinear optical susceptibility, enhanced redox activity, and conductivity;<sup>22,23</sup> the expansion of the C–C bonds of diamond would provide the so-called laboratory-grown diamond, which is predicted to be quite stable.<sup>24</sup>

Among the carbo compounds, carbo-cycloalkanes are probably the most widely studied to date. Carbo-cycloalkanes

Received: February 28, 2014

Published: May 20, 2014

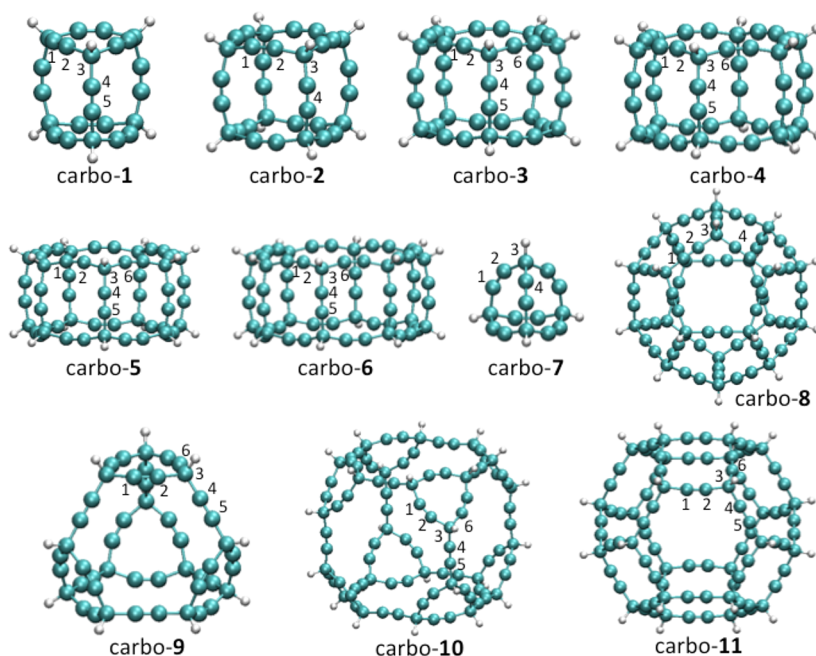


**Figure 1.** Optimized structures of  $(C_4H)_n$  carbo derivatives studied at the M06-2X/6-311G(d,p) level.

retain the symmetry, shape, and connectivity of the parent counterpart.<sup>25–27</sup> In the seminal work of Scott et al.,<sup>20,28</sup> a strong electronic coupling among acetylenic units was reported. Cyclic homoconjugation or homoaromaticity was suggested to be responsible for such an interaction. Since then, a significant amount of theoretical effort is devoted to unravel the properties of carbo-cycloalkanes.<sup>11,29,30</sup> Particular attention is paid to the changes in the ring strain and electron delocalization upon the insertion of  $C_2$  units. The incorporation of  $C_2$  moieties remarkably decreases strain due to the relaxation of bond angles;<sup>29,30</sup> then, stabilization of the carbomer structures will increase with the number of  $C_2$  units inserted in each C–C bond. Despite favorable geometric, energetic, and magnetic criteria, carbo-cycloalkanes are not homoaromatic.<sup>11,29</sup>

Synthesis of three-dimensional carbo structures remains a complicated challenge, mainly due to the instability of the intermediates. However, the interest in acetylenic cage compounds is notably increased since they serve as potential precursors of carbon fullerenes. In this framework, Manini et al. reported the synthesis of the expanded cubane, obtained by formal insertion of the  $C\equiv C-C\equiv C$  units into all 12 C–C bonds of a parent octamethoxy cubane.<sup>31</sup> Unfortunately, the latter compound is very unstable, exploding when scratched. It is expected that, upon ionization, the  $C_{56}$  core will lose the methoxy groups to immediately rearrange to a fullerene-like structure.

Some theoretical works are carried out to unveil the particular properties of alkynyl-expanded tetrahedrane, prismane, cubane, and adamantane.<sup>32–34</sup> In the same line, Jarowski et al. reported an *in silico* study of diacetylene (buta-1,3-diyne)–expanded platonic hydrocarbons.<sup>34</sup> A general conclusion is that the incorporation of  $C\equiv C$  units notably decreases the strain of the parent compounds. However, no systematic study, including several polyhedranes and platonic hydrocarbons, has been done in order to understand the metastability of the title compounds. In this article, we have analyzed systematically a series of cage hydrocarbons and their carbo derivatives via density functional theory (DFT)

computations, paying special attention to their structure, stability, heat of formation, ring strain, and aromaticity. Our benchmark study shows that the best level to describe the thermochemistry and structural properties of carbo-cages is the M06-2X functional in conjunction with a 6-311G(d,p) basis set. Using this approach, we have computed the strain energies, employing an adapted version of the homodesmotic reactions suggested by Wodrich et al. in order to match conjugation and hyperconjugation interactions as closely as possible.<sup>30</sup> Although our computations show that these carbo-cages have high heats of formation, one cannot rule out the probability of their future preparation and isolation since Born–Oppenheimer molecular dynamics simulations show that the systems are kinetically stable. This metastability is analyzed in terms of the electron delocalization, using the induced magnetic field analysis. The magnetic response is diatropic in nature around the three-membered rings, showing the presence of electron delocalization therein, whereas, for larger rings, the response is paratropic or close to zero, implying a nonaromatic behavior.

## ■ COMPUTATIONAL DETAILS

All geometries are fully optimized by means of the M06-2X<sup>35</sup> functional in conjunction with a 6-311G(d,p) basis set, as is implemented in the Gaussian 09 program package.<sup>36</sup> Harmonic vibrational frequencies are determined in order to ensure that the stationary points located are true minima of the corresponding potential energy surface and to compute the zero-point energy and thermal corrections.

The M06-2X functional accurately describes main-group thermochemistry, kinetics, noncovalent interactions, and electronic excitation energies of valence and Rydberg states.<sup>35</sup> Recently, using the same functional, a computational study of the ring strain energies of carbo-cycloalkanes was performed.<sup>30</sup> Nevertheless, to further guarantee the suitability of the results obtained with the M06-2X functional for the characterization of the title cage hydrocarbons and their carbomers, those are compared with the experimental work. Cubane is chosen as a model for this study because, to the best of our knowledge, it is the only polyhedrane with the available experimental data for enthalpy of formation. The calculated enthalpy of formation ( $154 \text{ kcal}\cdot\text{mol}^{-1}$ ) is comparable to the experimental data range (142.7 and 148.7 kcal

Table 1. Geometric Parameters of Selected Cage Hydrocarbons and Their Carbo Derivatives, Computed at the M06-2X/6-311G(d,p) Level<sup>f</sup>

	bond length					bond angle			
	C <sub>2</sub> -C <sub>3</sub>	C <sub>3</sub> -C <sub>4</sub>	C <sub>1</sub> ≡C <sub>2</sub>	C <sub>4</sub> ≡C <sub>5</sub>	C-H	C <sub>2</sub> -C <sub>3</sub> -C <sub>4</sub>	C <sub>2</sub> -C <sub>3</sub> -C <sub>6</sub>	C <sub>1</sub> ≡C <sub>2</sub> -C <sub>3</sub>	C <sub>3</sub> ≡C <sub>4</sub> -C <sub>5</sub>
carbo-1	1.486	1.477	1.203	1.198	1.091	107.4	100.5	157.4	165.4
1	1.514	1.550			1.080	90.0	60.0		
	<i>1.540<sup>a</sup></i>	<i>1.551<sup>a</sup></i>							
carbo-2	1.479		1.198		1.093		106.8	166.7	
2	1.562				1.087		90.0		
	<i>1.573<sup>b</sup></i>				<i>1.114<sup>b</sup></i>				
carbo-3	1.477	1.480	1.198	1.198	1.094	106.5	110.6	169.4	168.3
3	1.553	1.563			1.088	90.0	108.0		
	<i>1.548<sup>c</sup></i>	<i>1.565<sup>c</sup></i>							
carbo-4	1.476	1.480	1.198	1.198	1.095	106.4	113.5	168.9	169.4
4	1.553	1.559			1.089	90.0	120.0		
carbo-5	1.476	1.480	1.198	1.198	1.095	106.3	115.5	167.5	170.5
5	1.553	1.559			1.089	90.0	128.6		
carbo-6	1.475	1.479	1.198	1.198	1.096	106.3	117.0	166.1	171.4
6	1.557	1.558			1.091	90.0	135.0		
carbo-7	1.491		1.207		1.087		101.7	151.7	
7	1.471				1.069		60.0		
carbo-8	1.474		1.197		1.097		110.3	177.7	
8	1.549				1.091		108.0		
	<i>1.541<sup>d</sup></i>				<i>1.098<sup>e</sup></i>				
carbo-9	1.483	1.470	1.202	1.196	1.094	113.0	100.3	159.8	178.8
9	1.514	1.492			1.082	120.0	60.0		
carbo-10	1.482	1.468	1.202	1.197	1.096	116.0	100.6	159.3	174.2
10	1.532	1.515			1.094	135.0	60.0		
carbo-11	1.476	1.472	1.197	1.196	1.097	112.9	106.7	171.5	178.1
11	1.561	1.526			1.090	120.0	90.0		

<sup>a</sup>Reference 48. <sup>b</sup>Reference 49. <sup>c</sup>Reference 50. <sup>d</sup>Reference 51. <sup>e</sup>Reference 52. <sup>f</sup>Bond lengths are in Å, and angles are in degrees. Experimental data available are indicated in italics.

mol<sup>-1</sup>).<sup>37,38</sup> The computed C-C and C-H bonds are 1.573 and 1.114 Å, respectively, which match perfectly with the experimental values of 1.573 and 1.098 Å. Computations with other GGA (PBE, BLYP), meta-GGA (TPSS, M06-L), hybrid (PBE0, B3LYP), and meta-hybrid (M06) functionals are also performed (see Tables S1–S4 in the Supporting Information). GGA and hybrid functionals are unable to reproduce the experimental enthalpy of formation, whereas the values obtained using meta-GGA and meta-hybrid functionals are in good agreement with those of the experimentally obtained enthalpies of formation.

As one might notice from the data summarized in the Supporting Information, all the functionals employed here describe quite similarly the geometry of the title compounds. However, there are significant differences for the enthalpies of formation:

- GGA functionals (PBE, BLYP), in which the first-order gradient terms in the expansion are included, deliver the worst enthalpies of formation against the experimental numbers.
- The hybrid GGA functionals (PBE0, B3LYP), which incorporate a portion of the exact HF exchange to GGA, provide better values.
- Meta-GGA approaches (TPSS, TPSS-D2M06-L), which depend explicitly on the semilocal information in the Laplacian of the spin density or of the local kinetic energy density and imply a step further in the Jacob's ladder, are even closer to the experimental values.
- Meta-hybrid GGA approximations (M06, M06-2X), composed of meta-GGA functionals including a percentage of HF exchange, deliver the best agreement with the experimental values.

Since they sit in the fourth rung of the Jacob's ladder, M06 and M06-2X outperform the lower-lying GGA, hybrid GGA, and meta-GGA functionals. However, both M06 and M06-2X are heavily parametrized. The former was designed to describe organometallic compounds. The latter was optimized to characterize main-group chemistry and is better for the compounds considered in this work.

In addition, the induced magnetic field ( $B^{\text{ind}}$ )<sup>39–41</sup> is computed at the PW91/6-311G(d,p) level. The shielding tensors are calculated using the GIAO approach. Structures are placed in such a way that the center of the molecule is located at the origin of the coordinate system and the z axis is identical with the highest symmetry axis.

Born–Oppenheimer molecular dynamics (BOMD)<sup>42–45</sup> simulations are carried out using the deMon2k<sup>46</sup> program at the PBE/DZVP<sup>47</sup> level. The temperature of the canonical BOMD simulations is controlled by a Hoover chain thermostat. The simulations are started from the equilibrium geometry, with random velocities assigned to the atoms. For molecules 1–7 and 9, trajectories are recorded at 900 K. In the particular case of 1, BOMD simulations at 1200, 1500, and 2400 K are computed. All systems are sampled for 10 ps with a 1 fs step size.

## RESULTS AND DISCUSSION

**Structure and Stability.** Figure 1 depicts the optimized structures of carbo derivatives. Note that the shape and symmetry of the parent compounds are preserved (see Figure S1, Supporting Information). Selected bond lengths and bond angles of both the original cages and their carbomer counterparts are given in Table 1. The geometric parameters computed for the parent compounds are in excellent agreement with the corresponding experimental data<sup>48–52</sup> and with that obtained from previous high-level computations.<sup>1</sup> Deviations in bond lengths are within 0.01 Å, and bond angles essentially are

the same. C–C–C angles substantially differ from the ideal value of 109.5° in an sp<sup>3</sup>-hybridized C atom, leading to an important strain in the original polyhedranes. In the carbo derivatives, the single C–C bonds are significantly shorter than those computed for the parent compounds, in agreement with previous results on carbo-cycloalkanes.<sup>30</sup> Computed triple bond distances are 1.20–1.21 Å, in agreement with those reported by Wodrich et al.<sup>30</sup>

It is apparent from Figure 1 that all the carbo species display bowed edges. The insertion of the C<sub>2</sub> moieties produces a significant relaxation of the original C–C–C angles. The C≡C–C angles are computed giving a broad range between 151.4° (carbo-7) and 178.7° (carbo-11). Some of the C≡C–C angles notably differ from the ideal value of 180°, as previously reported for carbomer [*n*]-prismanes.<sup>53</sup> Most of the strain is concentrated in the acetylene units, and the energy penalty associated with the bending about a C(sp<sup>3</sup>) center is predicted to be significantly smaller than the one related to a deformation process.<sup>34</sup>

Table 2 summarizes the gas-phase enthalpies of formation, Δ<sub>f</sub>H°(g), for the cage hydrocarbons and their corresponding

**Table 2. Gas-Phase Standard State (298.15 K, 1 atm) Enthalpies of Formation (Δ<sub>f</sub>H°(g)) for the Selected Cage Hydrocarbons and Their Carbo Derivatives, Computed by Means of the Atomization Enthalpy Approach at the M06-2X/6-311G(d,p) Level<sup>a</sup>**

	polyhedrane	carbo-polyhedrane
1	135.2	651.0
2	154.4	816.2
	<i>142.7<sup>b</sup></i>	
	<i>148.7<sup>c</sup></i>	
3	133.3	1002.7
4	167.4	1202.0
5	224.9	1407.6
6	291.8	1617.3
7	121.9	477.5
8	50.6	1932.0
9	101.5	1249.8
10	370.2	2516.7
11	201.1	2350.8

<sup>a</sup>Enthalpies are given in kcal·mol<sup>-1</sup>. Experimental data available are indicated in italics. <sup>b</sup>Reference 37. <sup>c</sup>Reference 38.

carbo derivatives, computed by means of the atomization enthalpy approach.<sup>54</sup> The computed enthalpy of formation of 154 kcal·mol<sup>-1</sup> for cubane is in good agreement with the experimental values of 142.7<sup>37</sup> and 148.7 kcal·mol<sup>-1</sup>.<sup>38</sup> Moreover, the enthalpies of formation for the rest of the cage are in agreement with the high-level CBS-Q//B3, G4MP2, and G4 calculations, with relative errors of 5%, further confirming the suitability of the computational approach adopted here.<sup>1</sup> The computed enthalpies of atomization match with the values calculated on the basis of isodesmic and homodesmic reactions.<sup>1,37</sup> However, it is known that the latter approach could provide wrong numbers due to the uncertainty in the experimental data employed.<sup>1</sup>

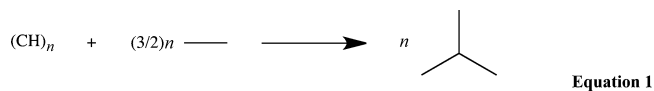
Dodecahedrane (8) is the most stable parent compound, with a Δ<sub>f</sub>H°(g) of 50.6 kcal·mol<sup>-1</sup> (see Figure 2). On the other hand, the truncated cubane (10) has the highest enthalpy of formation (370.2 kcal·mol<sup>-1</sup>). Among prismanes, pentaprismane is the most stable cage and triprismane is only 2 kcal·

mol<sup>-1</sup> higher in energy. For bigger prismanes, the stability decreases when the size of the compound increases. The insertion of the C≡C moieties produces a destabilization of the cage species, as previously reported by Wang and Zhang.<sup>53</sup> Interestingly, the formation energy of the carbo species changes notably with regard to their parent cages. For prismane-based carbomers, the enthalpy of formation increases proportionally to the size of the compound. Carbo-dodecahedrane is notably destabilized with regard to the original cage. Carbo-tetrahedrane is the most stable system in our set, with a computed Δ<sub>f</sub>H°(g) of 477.5 kcal·mol<sup>-1</sup>. The carbo derivative of the truncated cubane is the species with the highest enthalpy of formation, with a computed value of 2516.7 kcal·mol<sup>-1</sup>.

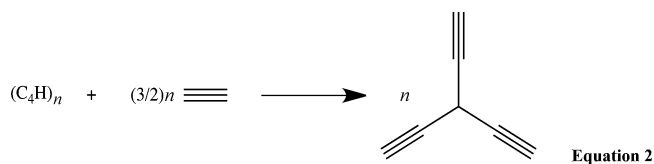
Carbomers show enthalpies of formation 1 order of magnitude higher, on average, than those obtained for their parent compounds. These values are close to that obtained for the octamethoxy expanded cubane synthesized by Manini et al.<sup>31</sup> (1241.7 kcal·mol<sup>-1</sup>). Again, carbomers result from the insertion of one or more –C≡C– units into the bonds of a parent compound. The simplest example of a carbomer is acetylene itself. The heat of formation of C<sub>2</sub>H<sub>2</sub> is positive. Its formation involves consumption of energy, and its decomposition releases the energy stored up in the molecule. Figure 3 shows a linear correlation between the number of C<sub>2</sub> units inserted in the cage with the changes of enthalpies of formation between the carbo-cages and the corresponding parent compounds. Therefore, clearly, the insertion of the C<sub>2</sub> units is the origin for such tremendous values of heat of formation. In other words, carbo-cages can be designed as explosives, explaining why the synthesized carbo-cubane exploded when scratched. In the particular case of carbo-dodecahedrane, it contains 30 C<sub>2</sub> units, so this is the reason why it has a so high heat of formation, but at the same time, the strain is reduced until 9 kcal/mol (vide infra).

**Strain Energy.** Strain energy represents an important concept specifically related to the release of energy, which may be responsible for many chemical transformations. Given that this is not an experimental observable, several approaches are proposed to quantify the strain energy. Most of them are based on chemical equations, where all structural and stereoelectronic features are balanced, except for the strain energy itself. Depending on the degree of bonding and hybridization, isogyric, isodesmic, hypohomodesmotic, homodesmotic, and hyperhomodesmotic equations are employed.<sup>30,55</sup>

The homodesmotic approach is probably the most widely employed to predict the conventional strain energies of cage hydrocarbons.<sup>1,6,7,30</sup> In this framework, the cage strain of a polyhedral hydrocarbon (CH)<sub>n</sub> is estimated as the energy change associated with eq 1:



Similarly (eq 2), it can be written to predict the strain energy of the corresponding carbo derivatives (C<sub>4</sub>H)<sub>n</sub>:



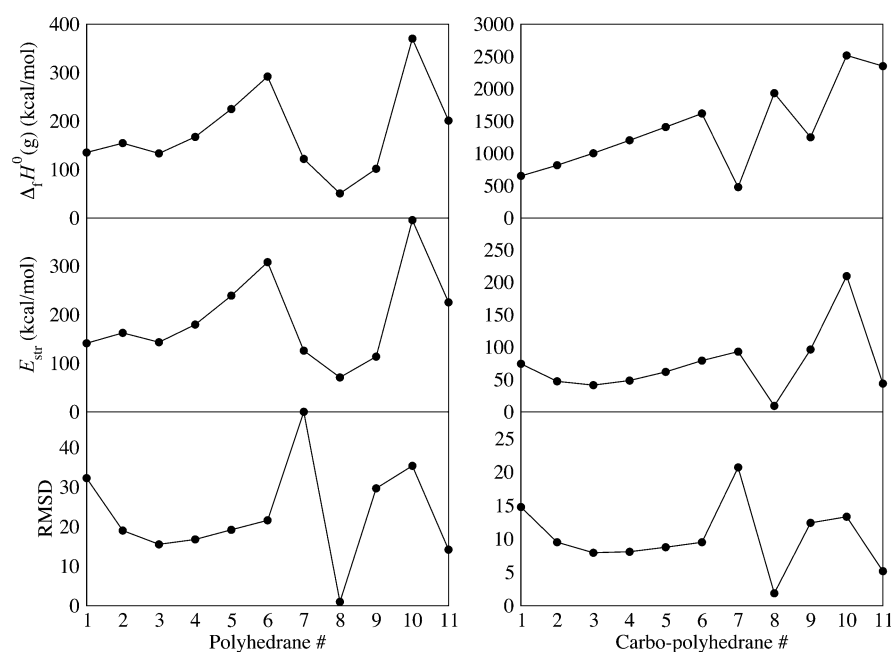


**Figure 2.** Estimated gas-phase standard state enthalpies of formation ( $\Delta_f H^\circ(g)$ ) and strain energies ( $E_{str}$ ) of polyhedranes and their carbo derivatives. Computations are performed as the enthalpy differences corresponding to the proposed homodesmotic equations. Values are obtained at the M06-2X/6-311G(d,p) level and are in kcal·mol<sup>-1</sup>. Root mean square deviations of the C–C–C and the C≡C–C angles are also shown.

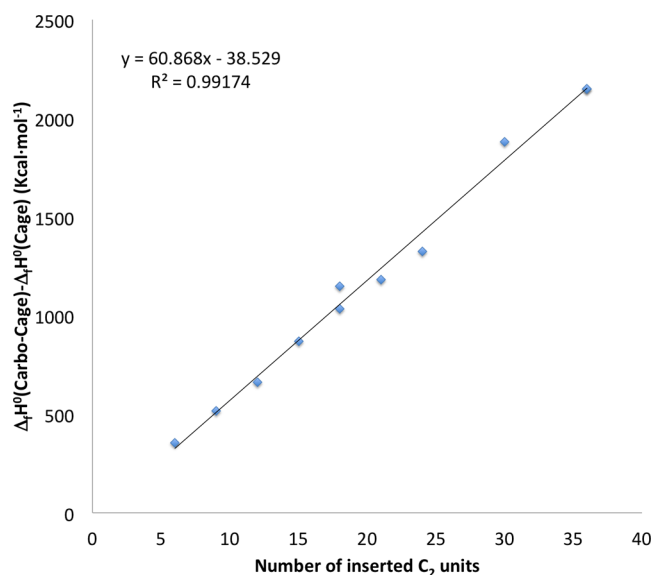


**Figure 3.** Correlation between the number of inserted C<sub>2</sub> units into the cages and the change of the heat of formation between the carbo-cages and the corresponding parent compounds.

Quite recently, these kinds of equations have succeeded in balancing all stereoelectronic effects present within carbo-cycloalkanes, allowing for a direct assessment of the strain energies.<sup>30</sup> Table 3 summarizes the strain energies for the title compounds, computed as the enthalpy difference associated with the homodesmotic equations proposed. It can be noticed from Table 3 and Figure 2 that the strain energies calculated for the parent polyhedranes essentially corroborate with their enthalpies of formation. In this sense, the strain seems to determine the stability of the considered species. The strain energy of 162.6 kcal·mol<sup>-1</sup> computed for cubane essentially coincides with the experimental determination of 166 kcal·mol<sup>-1</sup>.<sup>31</sup> Our computed values for [2,*n*]-prismanes are in

**Table 3.** Strain Energies ( $E_{str}$ ) for the Selected Cage Hydrocarbons and Their Carbo Derivatives at the M06-2X/6-311G(d,p) Level<sup>a</sup>

	Polyhedrane			Carbo-polyhedrane		
	(3 <i>n</i> )/2	<i>n</i>	$E_{str}$	(3 <i>n</i> )/2	<i>n</i>	$E_{str}$
1	9	6	141.31	9	6	74.20
2	12	8	162.55	12	8	47.10
3	15	10	143.46	15	10	41.34
4	18	12	179.57	18	12	48.38
5	21	14	239.15	21	14	61.72
6	24	16	308.11	24	16	79.10
7	6	4	125.98	6	4	92.96
8	30	20	70.97	30	20	9.22
9	18	12	113.70	18	12	96.15
10	36	24	394.61	36	24	209.45
11	36	24	225.47	36	24	43.52

<sup>a</sup>Energies are given in kcal·mol<sup>-1</sup>.

agreement with previous high-level calculations too.<sup>1</sup> Triprismane and tetrahedrane resulted surprisingly stable, given their acute bond angles. Indeed, the root mean square deviation (RMSD) of their C–C–C angles, calculated with respect to the ideal value of 109.5°, reveals a significant geometrical strain.

However, the development of  $\sigma$ -aromaticity in three-membered rings (and perhaps in five-membered rings, *vide infra*) stabilizes polyhedranes bearing trigonal (and perhaps pentagonal) faces.<sup>12</sup> Such delocalization is associated with strain energies.<sup>12</sup> The proposed homodesmotic equations were unable to decouple the strain energies from the rest of the contributions.<sup>30</sup>

The introduction of the  $C_2$  units results in a drastic lowering of the strain, as previously reported for cycloalkanes. Such reduction is presumably related to the relaxation of the C–C–C angles in the vertices of the cage. Consequently, the RMSDs of the C–C–C and the  $C\equiv C$ –C angles are much smaller. The strain energy implies only a small portion of the enthalpy of formation. Moreover, the strain does not fit the trend shown by the enthalpies of formation, in contrast to the parent polyhedranes. Carbo-dodecahedrane displays the lowest strain energy but a very large enthalpy of formation. Carbo-tetrahedrane is the most stable carbo-cage, despite showing a quite large strain energy, relative to the rest of the species. The RMSD curve essentially coincides with the trend given by the strain energy, suggesting that  $\sigma$ -aromaticity vanishes upon carbomerization, in agreement with previous results.<sup>30</sup>

**Kinetic Stability.** Now, the question is whether carbo-cages are at all stable to synthesize. As we know, the stability of a system depends on both thermodynamics and kinetics. From the values of the enthalpies of formation, it is obvious that carbo-cages are not thermodynamically stable, but still, we do not know how fast the systems undergo changes to convert into their corresponding more stable isomers.

In order to know if the systems are kinetically stable or not and thus if they are viable, we have performed a series of BOMD simulations at the PBE/DZVP level (except for **8**, **10**, and **11**). From the analysis of the structural evolution along the recorded trajectories, we note that all the systems maintain their structures at 900 K for 10 ps (see the movies in the Supporting Information).

In the particular case of **1**, BOMD simulations at 1200, 1500, and 2400 K for 10 ps are computed. Until 2400 K, we have not seen any structural change in the carbon skeleton. At 2400 K, a single C–C bond is broken and a complex structural change is started. Therefore, the systems are kinetically stable and hence are viable.

**Aromaticity.** In order to understand electron delocalization, the magnetic response to an external magnetic field was analyzed.<sup>39–41</sup> This response will depend on the magnitude and direction of the external field ( $B^{ext}$ ). Profiles of the  $z$ -component of the induced magnetic field bisecting ring planes provide more details (see Figure 4 and Table 4). Magnitudes are shown by the size of the spheres. For comparison, the parent cages are also computed.

Clearly, the magnetic response around the three-membered ring (3MR), in both the parents and the carbo compounds, is diatropic; i.e., they can be considered as aromatic. The values at the 3MRs are around  $-10$  ppm. In contrast, for larger rings (4–7MRs), the response is paratropic or close to zero. The magnitude of the extreme values is not extremely high (less than 10 ppm). Usually, the  $B_z^{ind}$  value for antiaromatic systems is larger. Cyclobutadiene, the archetypal antiaromatic compound, shows a strong paratropic behavior with a  $B_z^{ind}(0)$  of 109 ppm. Then, the induced magnetic field indicates a nonaromatic behavior, rather than an antiaromatic response. Carbo-prismane (carbo-**1**) and its parent compound (**1**) are special cases: they have a competing diatropic 3MRs and

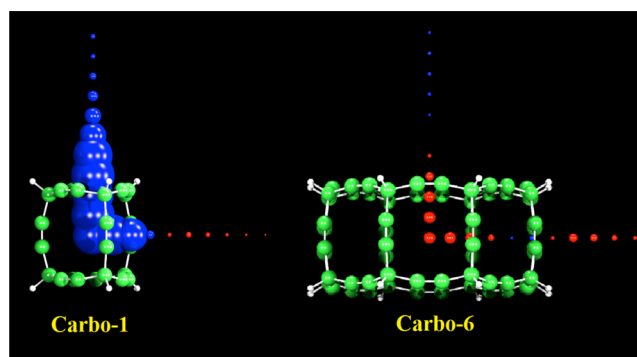


**Figure 4.**  $B_z^{ind}$  profiles. Red and blue spheres denote positive and negative values, respectively.

nonaromatic 4MRs responses. This is also evident in carbo-**9** and carbo-**10**. The strongest diatropic response is exhibited by carbo-tetrahedrane ( $-13.2$  ppm), but it is almost half of that computed for its parent analogue.

If one compares each carbomer with its parent compound (see Table 2), it is apparent that the values are shifted,<sup>12</sup> but the aromatic or nonaromatic character is preserved. This fact is in agreement with the assumption that carbo compounds will retain symmetry, shape, and properties of the parent counterpart, including aromaticity.

## CONCLUSIONS

Polyhedranes are characterized by their highly strained geometry, with C–C–C bond angles that often differ from the ideal value of  $109.5^\circ$  in an  $sp^3$ -hybridized C atom. The insertion of the  $C_2$  units produces a significant relaxation of the original C–C–C angles. Concomitant with this structural rearrangement is the shortening of the parent C–C bonds. The  $C\equiv C$ –C angles are significantly bent, meaning that most of the strain in the carbo compounds is concentrated in the acetylene units. The parent polyhedranes possess larger strain energies. Moreover, the strain seems to determine the stability of the compound. The introduction of the alkynyl units results in a significant lowering of the strain, due to the relaxation of the C–C–C angles in the vertices of the cage.

The carbo derivatives have enthalpies of formation 1 order of magnitude higher than those of their parent compounds. A linear correlation exists between the number of  $C_2$  units inserted in the cage with the changes of enthalpies of formation between the carbo-cages and the parent compounds. Therefore, clearly, the insertion of the  $C_2$  units is the origin for such tremendous values of heat of formation. Nevertheless, the BOMD simulations show that all the systems maintain their structures at 900 K for 10 ps. In the particular case of **1**, BOMD simulations at 1200, 1500, and 2400 K for 10 ps are computed. Until 2400 K, we have not seen any structural change in the carbon skeleton. At 2400 K, a single C–C bond is broken and a complex structural change is started. Therefore, the systems are kinetically stable and hence are viable.

Regarding electron delocalization of cage polyhedranes, the magnetic response around the three-membered rings is found to be diatropic; i.e., they can be considered as aromatic. For larger rings, the response is paratropic or close to zero, indicating a nonaromatic behavior. Upon carbomerization, the values of the magnetic response are shifted, but the aromatic/nonaromatic character is preserved.

Table 4.  $B_z^{\text{ind}}$  (in ppm) at Cage and Ring Centers Computed at the PW91/6-311G(d,p)//M06-2X/6-311G(d,p) Level

centers		$B_z^{\text{ind}}$		$B_z^{\text{ind}}$	centers		$B_z^{\text{ind}}$		$B_z^{\text{ind}}$
cage	carbo-1	-10.1	1	-50.5	cage	carbo-6	2.9	6	1.2
3MR (0)		-10.4		-42.8	8MR (0)		2.7		3.3
3MR (1)		-11.0		-30.0	8MR (1)		1.8		-2.5
4MR (0)		-10.3		-53.2	4MR (0)		-1.8		-25.3
4MR (1)		-6.2		-4.6	4MR (1)		0.7		1.4
cage	carbo-2	4.3	2	25.1	cage	carbo-7	-12.6	7	-35.4
4MR (0)		11.3		59.3	3MR (0)		-13.1		-32.7
4MR (1)		6.4		8.5	3MR (1)		-13.2		-22.6
cage	carbo-3	2.0	3	-5.9	cage	carbo-8	0.4	8	0.8
5MR (0)		4.8		9.2	5MR (0)		5.3		24.5
5MR (1)		2.5		-9.9	5MR (1)		2.6		-3.3
4MR (0)		-2.6		-32.5	cage	carbo-9	-0.9	9	-16.2
4MR (1)		-0.5		-1.4	6MR (0)		4.5		5.9
cage	carbo-4	3.1	4	0.8	6MR (1)		3.3		-6.6
6MR (0)		4.2		10.7	3MR (0)		-9.1		-31.7
6MR (1)		2.6		-3.0	3MR (1)		-10.5		-26.0
4MR (0)		-2.0		-25.0	cage	carbo-10	-0.2	10	-5.2
4MR (1)		0.1		1.5	8MR (0)		3.5		15.5
cage	carbo-5	3.1	5	18.8	8MR (1)		2.9		6.6
7MR (0)		3.2		22.7	3MR (0)		-8.3		-39.7
7MR (1)		2.1		7.4	3MR (1)		-5.5		-5.2
4MR (0)		-1.8		-14.5	cage	carbo-11	1.0	11	-1.5
4MR (1)		0.5		0.2	6MR (0)		0.5		-2.7
					6MR (1)		0.2		-2.2
					4MR (0)		11.9		60.0
					4MR (1)		6.3		2.7

## ■ ASSOCIATED CONTENT

### ■ Supporting Information

The geometries of the parent polyhedranes and enthalpies of formation and geometrical parameters of cubane and carbo-cubane computed using different functionals. Born–Oppenheimer molecular dynamics simulation movies at 900 K for carbo-1 to carbo-9 in mp4 format are provided in a compressed zip file. This material is available free of charge via the Internet at <http://pubs.acs.org>.

## ■ AUTHOR INFORMATION

### ■ Corresponding Authors

\*E-mail: [gmerino@mda.cinvestav.mx](mailto:gmerino@mda.cinvestav.mx) (G.M.).

\*E-mail: [jesus.ugalde@ehu.es](mailto:jesus.ugalde@ehu.es) (J.M.U.).

### ■ Notes

The authors declare no competing financial interest.

## ■ ACKNOWLEDGMENTS

The authors gratefully thank Conacyt (Grants 176863 and INFRA-2013-01-204586) and VIEP-BUAP (Grant VIEP-098-2014). Moshinsky Foundation supported the work in Mérida. The CGSTIC (Xiuhcoalt) at Cinvestav is gratefully acknowledged for generous allocation of computational resources. Technical and human resources provided by IZO-SGI, SGIker (UPV/EHU, MICINN, GV/EJ, ERDF and ESF) are gratefully acknowledged. Financial support through Grant REA-FP7-IRSES TEMM1P (GA 295172) is also acknowledged. P.K.C. would like to thank DST, New Delhi, for the J. C. Bose National Fellowship, and S.P. thanks CSIR, New Delhi, for his fellowship.

## ■ REFERENCES

- (1) Rayne, S.; Forest, K. *Theor. Chem. Acc.* **2010**, *127*, 697.
- (2) Earley, C. W. *J. Phys. Chem. A* **2000**, *104*, 6622.
- (3) Gonthier, J. F.; Steinmann, S. N.; Wodrich, M. D.; Corminboeuf, C. *Chem. Soc. Rev.* **2012**, *41*, 4671.
- (4) Moran, D.; Woodcock, H. L.; Chen, Z.; Schaefer, H. F.; Schleyer, P. v. R. *J. Am. Chem. Soc.* **2003**, *125*, 11442.
- (5) Nemirowski, A.; Reisenauer, H. P.; Schreiner, P. R. *Chem.—Eur. J.* **2006**, *12*, 7411.
- (6) Tan, B.; Long, X.; Li, J. *Comput. Theor. Chem.* **2012**, *993*, 66.
- (7) Walker, J. E.; Adamson, P. a.; Davis, S. R. *J. Mol. Struct.: THEOCHEM* **1999**, *487*, 145.
- (8) Wu, H.-S.; Qin, X.-F.; Xu, X.-H.; Jiao, H.; Schleyer, P. v. R. *J. Am. Chem. Soc.* **2005**, *127*, 2334.
- (9) Pelloni, S.; Carion, R.; Liégeois, V.; Lazzarretti, P. *J. Comput. Chem.* **2011**, *32*, 1599.
- (10) De Proft, F.; Geerlings, P. *Chem. Rev.* **2001**, *101*, 1451.
- (11) Lepetit, C.; Silvi, B.; Chauvin, R. *J. Phys. Chem. A* **2003**, *107*, 464.
- (12) Moran, D.; Manoharan, M.; Heine, T.; Schleyer, P. v. R. *Org. Lett.* **2003**, *5*, 23.
- (13) Jefford, C. W. *J. Chem. Educ.* **1976**, *53*, 477.
- (14) Hare, M.; Emrick, T.; Eaton, P. E.; Kass, S. R. *J. Am. Chem. Soc.* **1997**, *119*, 237.
- (15) Katz, T. J.; Acton, N. *J. Am. Chem. Soc.* **1973**, *95*, 2738.
- (16) Eaton, P. E.; Cole, T. W. *J. Am. Chem. Soc.* **1964**, *86*, 3157.
- (17) Barborak, J. C.; Watts, L.; Pettit, R. *J. Am. Chem. Soc.* **1966**, *88*, 1328.
- (18) Eaton, P. E.; Or, Y. S.; Branca, S. J. *J. Am. Chem. Soc.* **1981**, *103*, 2134.
- (19) Eaton, P. E.; Or, Y. S.; Branca, S. J.; Shankar, B. K. R. *Tetrahedron* **1986**, *42*, 1621.
- (20) Scott, L. T.; DeCicco, G. J.; Hyun, J. L.; Reinhardt, G. J. *Am. Chem. Soc.* **1983**, *105*, 7760.
- (21) Boldi, A. M.; Diederich, F. *Angew. Chem., Int. Ed. Engl.* **1994**, *33*, 468.

- (22) Baughman, R. H.; Eckhardt, H.; Kertesz, M. *J. Chem. Phys.* **1987**, *87*, 6687.
- (23) Haley, M. M.; Brand, S. C.; Pak, J. J. *Angew. Chem.* **1997**, *36*, 836.
- (24) Diederich, F.; Rubin, Y. *Angew. Chem., Int. Ed. Engl.* **1992**, *31*, 1101.
- (25) Maurette, L.; Godard, C.; Frau, S.; Lepetit, C.; Soleilhavoup, M.; Chauvin, R. *Chem.—Eur. J.* **2001**, *7*, 1165.
- (26) Leroyer, L.; Lepetit, C.; Rives, A.; Maraval, V.; Saffon-Merceron, N.; Kandaskalov, D.; Kieffer, D.; Chauvin, R. *Chem.—Eur. J.* **2012**, *18*, 3226.
- (27) Lepetit, C.; Zou, C. H.; Chauvin, R. *J. Org. Chem.* **2006**, *71*, 6317.
- (28) Scott, L. T.; DeCicco, G. J.; Hyun, J. L.; Reinhardt, G. *J. Am. Chem. Soc.* **1985**, *107*, 6546.
- (29) Jiao, H.; van Eikema Hommes, N. J. R.; Schleyer, P. v. R.; de Meijere, A. *J. Org. Chem.* **1996**, *61*, 2826.
- (30) Wodrich, M. D.; Gonthier, J. F.; Steinmann, S. N.; Corminboeuf, C. *J. Phys. Chem. A* **2010**, *114*, 6705.
- (31) Manini, P.; Amrein, W.; Gramlich, V.; Diederich, F. *Angew. Chem., Int. Ed. Engl.* **2002**, *41*, 4339.
- (32) Bachrach, S. M. *J. Phys. Chem. A* **2003**, *107*, 4957.
- (33) Bachrach, S. M.; Demoin, D. W. *J. Org. Chem.* **2006**, *71*, 5105.
- (34) Jarowski, P. D.; Diederich, F.; Houk, K. N. *J. Org. Chem.* **2005**, *70*, 1671.
- (35) Zhao, Y.; Truhlar, D. G. *Theor. Chem. Acc.* **2007**, *120*, 215.
- (36) Frisch, M. J.; Trucks, G. W.; Schlegel, H. B.; Scuseria, G. E.; Robb, M. A.; Cheeseman, J. R.; Scalmani, G.; Barone, V.; Mennucci, B.; Petersson, G. A.; Nakatsuji, H.; Caricato, M.; Li, X.; Hratchian, H. P.; Izmaylov, A. F.; Bloino, J.; Zheng, G.; Sonnenberg, J. L.; Hada, M.; Ehara, M.; Toyota, K.; Fukuda, R.; Hasegawa, J.; Ishida, M.; Nakajima, T.; Honda, Y.; Kitao, O.; Nakai, H.; Vreven, T.; Montgomery, J. A., Jr.; Peralta, J. E.; Ogliaro, F.; Bearpark, M.; Heyd, J. J.; Brothers, E.; Kudin, K. N.; Staroverov, V. N.; Kobayashi, R.; Normand, J.; Raghavachari, K.; Rendell, A.; Burant, J. C.; Iyengar, S. S.; Tomasi, J.; Cossi, M.; Rega, N.; Millam, N. J.; Klene, M.; Knox, J. E.; Cross, J. B.; Bakken, V.; Adamo, C.; Jaramillo, J.; Gomperts, R.; Stratmann, R. E.; Yazyev, O.; Austin, A. J.; Cammi, R.; Pomelli, C.; Ochterski, J. W.; Martin, R. L.; Morokuma, K.; Zakrzewski, V. G.; Voth, G. A.; Salvador, P.; Dannenberg, J. J.; Dapprich, S.; Daniels, A. D.; Farkas, Ö.; Foresman, J. B.; Ortiz, J. V.; Cioslowski, J.; Fox, D. J. *Gaussian 09*; Gaussian Inc.: Wallingford, CT, 2009.
- (37) Karpushenkava, L. S.; Kabo, G. J.; Bazyleva, A. B. *J. Mol. Struct.: THEOCHEM* **2009**, *913*, 43.
- (38) Kybett, B. D.; Carroll, S.; Natalis, P.; Bonnell, D. W.; Margrave, J. L.; Franklin, J. L. *J. Am. Chem. Soc.* **1966**, *88*, 2267.
- (39) Heine, T.; Islas, R.; Merino, G. *J. Comput. Chem.* **2007**, *28*, 302.
- (40) Islas, R.; Heine, T.; Merino, G. *Acc. Chem. Res.* **2012**, *45*, 215.
- (41) Merino, G.; Heine, T.; Seifert, G. *Chem.—Eur. J.* **2004**, *10*, 4367.
- (42) Bolton, K.; Hase, W. L.; Peshlherbe, G. H. *Modern Methods for Multidimensional Dynamics Computation in Chemistry*; World Scientific: Singapore, 1998.
- (43) Chen, W.; Hase, W. L.; Schlegel, H. B. *Chem. Phys. Lett.* **1994**, *228*, 436.
- (44) Millam, J. M.; Bakken, V.; Chen, W.; Hase, W. L.; Schlegel, H. B. *J. Chem. Phys.* **1999**, *111*, 3800.
- (45) Li, X. S.; Millam, J. M.; Schlegel, H. B. *J. Chem. Phys.* **2000**, *113*, 10062.
- (46) Koster, A. M.; Geudtner, G.; Calaminici, P.; Casida, M. E.; Dominguez, V. D.; Flores-Moreno, R.; Gamboa, G. U.; Goursot, A.; Heine, T.; Ipatov, A.; Janetzko, F.; del Campo, J. M.; Reveles, J. U.; Vela, A.; Zuniga-Gutierrez, B.; Salahub, D. R. *deMon2k*, Version 3; Cinvestav: Mexico City, Mexico, 2011.
- (47) Godbout, N.; Salahub, D. R.; Andzelm, J.; Wimmer, E. *Can. J. Chem.* **1992**, *70*, 560.
- (48) Karl, R. R., Jr.; Wang, Y. C.; Bauer, S. H. *J. Mol. Struct.* **1975**, *25*, 17.
- (49) Bischof, P.; Eaton, P. E.; Gleiter, R.; Heilbronner, E.; Jones, T. B.; Schmelzer, A.; Stober, R. *Helv. Chim. Acta* **2004**, *61*, 547.
- (50) Engel, P.; Eaton, P. E.; Shankar, B. K. R. *Z. Kristallogr.* **1982**, *159*, 239.
- (51) Paquette, L. A.; Balogh, D. W.; Usha, R.; Kountz, D.; Christoph, G. G. *Science* **1981**, *211*, 575.
- (52) Christoph, G. G.; Engel, P.; Usha, R.; Balogh, D. W.; Paquette, L. A. *J. Am. Chem. Soc.* **1982**, *104*, 784.
- (53) Wang, Z.; Zhang, J. *Chin. J. Struct. Chem.* **2011**, *30*, 1367.
- (54) Saeys, M.; Reyniers, M.-F.; Marin, G. B.; Van Speybroeck, V.; Waroquier, M. *J. Phys. Chem. A* **2003**, *107*, 9147.
- (55) Wheeler, S. E.; Houk, K. N.; Schleyer, P. v. R.; Allen, W. D. *J. Am. Chem. Soc.* **2009**, *131*, 2547.